Quaternary Science Reviews 304 (2023) 108009

Contents lists available at ScienceDirect

Quaternary Science Reviews

journal homepage: www.elsevier.com/locate/quascirev

Periodicity of the Southern Annular Mode in Southern Patagonia, insight from the Lago Argentino varve record

Maximillian Van Wyk de Vries [a, b, c, d, *], Emi Ito [a], Matias Romero [e, f, g], Mark Shapley [h], Guido Brignone [e]

[a] Limnological Research Center, Department of Earth and Environmental Sciences, University of Minnesota, Minneapolis, MN, 55455, USA
[b] Saint Anthony Falls Laboratory, University of Minnesota, Minneapolis, MN, 55455, USA
[c] School of Environmental Sciences, University of Liverpool, Liverpool, L3 5DA, UK
[d] School of Geography and the Environment, University of Oxford, Oxford, OX1 3QY, UK
[e] Facultad de Ciencias Exactas, Físicas y Naturales (FCEFyN), Universidad Nacional de Córdoba, Av. Haya de la Torre, Córdoba, X5000HUA, Argentina
[f] Centro de Investigaciones en Ciencias de la Tierra (CICTERRA), Consejo Nacional de Investigaciones Científicas y Tecnológicas (CONICET), Córdoba, X5000IND, Argentina
[g] Department of Geoscience, University of Wisconsin-Madison, Madison, WI, 53706, USA
[h] Continental Scientific Drilling Facility, Dept. of Earth and Environmental Sciences, University of Minnesota, Minneapolis, MN, 55455, USA

ARTICLE INFO

Article history:
Received 28 July 2022
Received in revised form
4 February 2023
Accepted 13 February 2023
Available online 20 February 2023

Handling editor: Claudio Latorre

Keywords:
Southern Annular Mode
Patagonia
Paleoclimate
Spectral analysis
Lago Argentino
lake core

ABSTRACT

Climatic variability across a large fraction of the Southern Hemisphere is controlled by the Southern Annular Mode and associated latitudinal shifts in the Southern Westerly Wind belt. In Patagonia, these changes control the large-scale temperature and precipitation trends – and resulting glacier surface mass balance. Our understanding of recent changes in this climatic oscillation is, however, limited by the number of paleo-environmental records in the mid to high-latitude Southern Hemisphere. Here, we first use a synthetic proxy record to demonstrate that periodicity may be preserved in a wider range of records than can be used for quantitative paleoclimatic reconstructions. We then analyze a 5000-year-long sedimentation record derived from Lago Argentino, a 1500 km^2 ice-contact lake in Southern Patagonia. We extract a mass accumulation rate and greyscale pixel intensity record from 28 cores across all of Lago Argentino's main depositional environments. We align the mass accumulation rate and pixel intensity records to a common time axis through multivariate dynamic-time-warping, and investigate their spectral properties using the multi-taper Lomb Scargle periodogram. We find statistically significant spectral peaks at 200 ± 20, 150 ± 16, and 85 ± 9 years in two thirds of mass accumulation rate and one third of the pixel intensity records. These periodicities reveal the centennial periodicity of the Southern Annular Mode, which is the key climatic driver of sedimentation at Lago Argentino.

© 2023 The Authors. Published by Elsevier Ltd. This is an open access article under the CC BY license (http://creativecommons.org/licenses/by/4.0/).

1. Introduction

Climatic variability in the high-latitudes of the Southern Hemisphere is a key component of the global climate system (Abram et al., 2014; Fogt and Marshall, 2020; Perren et al., 2020). The dominant mode of climatic variability in the extratropical Southern Hemisphere is the Southern Annular Mode (SAM), which controls the displacement of atmospheric mass between the mid-latitudes and Antarctica (Hessl et al., 2017; Marshall, 2003; Visbeck, 2009), and may be measured as the pressure difference between these locations (Hessl et al., 2017; Marshall, 2003; Saunders et al., 2017; Visbeck, 2009). Changes in the SAM also determine the latitudinal position of the primary westerly wind belt encircling Antarctica (Abram et al., 2014; Fogt and Marshall, 2020; Moreno et al., 2014). Variations in the SAM have wide-ranging implications for many critical Southern Hemisphere systems, including the strength of the Antarctic Circumpolar Current and oceanic mixing (Fogt and Marshall, 2020), Southern Ocean primary productivity (Hauck et al., 2013), polar warming and the stability of the Antarctic ice sheet margins (Marshall et al., 2006; Perren et al., 2020), and precipitation across the Southern

* Corresponding author. Water Lab, School of Geography and the Environment, S Parks Road, Oxford, OX1 3QY, UK.
E-mail address: maximillian.vanwykdevries@ouce.ox.ac.uk (M. Van Wyk de Vries).

https://doi.org/10.1016/j.quascirev.2023.108009
0277-3791/© 2023 The Authors. Published by Elsevier Ltd. This is an open access article under the CC BY license (http://creativecommons.org/licenses/by/4.0/).

Hemisphere (Moreno et al., 2014; Neukom and Gergis, 2012; Perren et al., 2020).

The core of the Southern Westerly Wind (SWW) belt intersects with the Patagonian Andes around 45°S to 50°S, resulting in extremely high precipitation values on the western flank of the Andes (Garreaud et al., 2012), while eastern Patagonia is arid due to a strong rain shadow effect (Garreaud et al., 2012; Richter et al., 2016). SAM-related latitudinal fluctuations in the position of the SWW belt affect both precipitation and temperature across Patagonia: poleward motion of the SWW belt is associated with strengthening of the wind system and warming across Patagonia (positive SAM phase), while equatorward motion of the SWW belt is associated with a reduction in wind speed and cooling (negative SAM phase; (Garreaud et al., 2009; Moreno et al., 2014; Reynhout et al., 2019; Villalba et al., 2012). A positive SAM phase also increases precipitation west of the Andean orographic divide and decreases it east of the divide, while SAM-negative phases result in drying west of the spine of the Andes and increased precipitation to the east (Garreaud et al., 2012; Reynhout et al., 2019). A late 20th and 21st century drying trend across much of Argentinian Patagonia has been associated with a present-day positive SAM phase (Aravena and Luckman, 2009; Garreaud et al., 2012).

Changes in temperature and precipitation affect glacier surface mass balance (Hock, 2005), and changes in SAM phase have tentatively been associated with episodes of glacier advance and recession in the Patagonian Icefields (Kaplan et al., 2016; Reynhout et al., 2019). Patagonia's location makes it particularly sensitive to the climatic shifts associated with the SAM, and an ideal location to identify proxy records of past Southern Hemisphere climatic variability.

High-quality instrumental climate records are only available in Patagonia for the past ~100 years (Marshall, 2003), and hence long-term paleoclimate reconstructions necessarily rely on proxies. Paleoclimatic proxies can be any sedimentary, biological, or compositional dataset which preserves information about the environmental conditions under which it was formed or deposited. The majority of paleoclimate proxy research has been focussed on the Northern Hemisphere, but a number of studies have investigated mid to late Holocene Patagonian climate (Lara et al., 2020; Massaferro and Larocque-Tobler, 2013; Villalba et al., 2012). Three main categories of paleoclimatic proxies in Patagonia are: tree rings, lacustrine or fjord sediment, and moraines.

Tree ring width reflects changes in the climatic variable most limiting to tree growth in the local area - typically temperature or precipitation (Villalba et al., 2012). Relative tree ring width (tree ring index) has been used to reconstruct maximum summer temperature over the past 5000 years in northern Patagonia (Lara et al., 2020), and correlate with SAM phase (Villalba et al., 2012). While tree rings are relatively widespread and provide an annual resolution proxy, most records are chronologically limited to the past few centuries.

Lacustrine or marine fjord sediment allows for several different types of climatic reconstruction, either through the properties or quantity of sediment itself (e.g., Elbert et al., 2015, 2012), or through the preservation of climatically-sensitive data within the sediment (e.g., (Caniupán et al., 2014; Davis, 1969; Massaferro and Larocque-Tobler, 2013; Moreno et al., 2014). Where the conditions are favorable, such proxy records may extend the entire Holocene or even into the last glacial period (Caniupán et al., 2014; Massaferro and Larocque-Tobler, 2013). Sediment mass accumulation rate (Elbert et al., 2012) and optical brightness (Elbert et al., 2015) have been used to reconstruct temperature and precipitation in various Patagonian lakes. Pollen records have been correlated with the Holocene temperature record and SAM cyclicity (Moreno et al., 2014). Massaferro and Larocque-Tobler (2013) reconstructed Holocene mean annual air temperature using a chironomid transfer function at Laguna Potrok Aike. Caniupán et al. (2014) used alkenones extracted from Chilean fjord sediment to reconstruct Holocene sea surface temperatures, while Lamy et al. (2001) used terrigenous sediment input to unravel Holocene rainfall variability induced by the latitudinal shifts of the SWW belt in southern Chile. Patagonian sediment records a range of valuable paleoclimatic information, but distributed across different climatic variables, timescales, and temporal resolutions.

Glaciers are sensitive to climatic variations, and glacial landforms indirectly preserve information about past climate (Leger et al., 2021). Many Patagonian glaciers record multiple past advances through frontal moraines (Davies et al., 2020; Kaplan et al., 2016; Reynhout et al., 2019; Strelin et al., 2014), corresponding to times of higher precipitation or lower temperatures. Numerical modeling of past glacier extents under a suite of different climatic scenarios has been used to quantitatively constrain past precipitation and temperature ranges (Leger et al., 2021), although qualitative correlations between glacier extent and climatic conditions are more common (Kaplan et al., 2016; Strelin et al., 2014; Warren, 1993). Reynhout et al. (2019) proposed that variations in SAM phase have paced Holocene glacier fluctuations in Patagonia by controlling the local precipitation and temperature. Glaciers only indirectly record past climate through the conditions favorable for glacier advance (high precipitation and/or low temperature), but provide one of the most extensive paleoenvironmental records in Patagonia.

Understanding the past evolution of the SAM in Patagonia is important for our present-day understanding of large-scale climatic controls on the region, and for forecasting future temperature and precipitation changes. Despite this, our understanding of the multidecadal to centennial variability in the SAM and the position of the SWW is limited. Many of the longer time series of paleoclimate, for instance the chironomid transfer function or alkenone-based temperature reconstructions (Caniupán et al., 2014; Massaferro and Larocque-Tobler, 2013), have insufficient temporal resolution to investigate centennial changes. Many of the higher temporal resolution datasets, for instance lacustrine varve (Elbert et al., 2015) or tree ring-based studies (Villalba et al., 2012), only extend back a few hundred years. Studies with both a high temporal resolution and temporal coverage greater than 1000 years (Abram et al., 2014; Elbert et al., 2012; Lara et al., 2020; Moreno et al., 2014) show limited agreement, and are too spatially far apart for a consensus Patagonian paleoclimate reconstruction. Our best understanding of past SAM changes comes from an agreement between Southern Patagonian pollen assemblage changes (Moreno et al., 2014) and glacial fluctuations (Kaplan et al., 2016; Reynhout et al., 2019; Strelin et al., 2014), which suggest an approximately 200-year duration of SAM-positive phases.

In this study, we used a large dataset of annually laminated lacustrine cores from Lago Argentino, a large Patagonian proglacial lake, to investigate paleoclimate periodicity in Southern Patagonia over the past 5000 years. We first used a synthetic proxy record to demonstrate that periodicity may be preserved in proxy records even where direct paleoclimatic reconstruction is not possible, and then investigated the spectral properties of the relative mass accumulation rate (rMAR) and greyscale pixel intensity (PxI) records of Lago Argentino. We then considered whether the rMAR or PxI spectra record any dominant periodicity related to the SAM or other large-scale climatic systems.

2. Setting

Lago Argentino is an ultra-oligotrophic, ice-contact lake located on the eastern flank of the Southern Patagonian Icefield (SPI) at

50°2′S, 72°4′W (Fig. 1). Lago Argentino has a surface area of around 1500 km^2 and is up to 600 m deep (Sugiyama et al., 2016). Two major rivers are located at the east of the main lake basin, one of which flows into the lake (Río La Leona), while the other drains the lake to the Atlantic Ocean (Río Santa Cruz). Six glaciers feed into Lago Argentino, of which three (Upsala, Perito Moreno and Spegazzini) calve directly into the lake and three calve into smaller peripheral lakes (Fig. 1). The main basin of the lake has remained free of glacial ice since at least 10 ka (Davies et al., 2020; Strelin et al., 2011). Precipitation is as high as several metres of water equivalent per year on the SPI itself, but due to a rain shadow effect the landscape surrounding Lago Argentino is semiarid and receives less than 500 mm of precipitation per year (Garreaud et al., 2012). Precipitation, temperature, and wind speed all vary seasonally, and local winds are dominantly westerlies related to the SWW belt, with 70% of measured wind directions in the range 230–320° (SW-NW). Positive SAM phases are associated with warming and drying across the Lago Argentino glacier catchment area, while negative SAM phases are associated with cooling and increases in precipitation (Garreaud et al., 2009; Reynhout et al., 2019).

3. Methods

3.1. Core collection and imaging

We collected 47 lake cores from Lago Argentino in Austral winter 2019. Twenty-five of these cores were collected using a specially adapted deep-water Kullenberg piston corer with 250–450 kg head weight, and a further 22 were collected using a gravity surface corer (Van Wyk de Vries et al., 2022, 2021). Where possible, both Kullenberg and gravity cores were collected at the same location. Our core distribution covers the main depositional environments of Lago Argentino. Following collection, we split, cleaned, and collected 20 μm per pixel line-scan imagery of each core (Van Wyk de Vries et al., 2022, 2021).

We selected a subset of 18 Kullenberg piston cores and 10 surface gravity cores from this dataset based on their degree of preservation and the presence of varves. Half of the piston cores are from the main lake basin and the other half are from the brazos, while 4 surface gravity cores are from the main lake basin and 6 are from the brazos. We remove event deposits from our dataset, with the remaining varved sediment exhibiting very minor down-core variability (Van Wyk de Vries et al., 2022). In addition, whole-core gamma-ray density scans do not show any systematic down-core density variations, with the exception of event deposits. Therefore, we assumed no down-core density variations and converted each core's sedimentation rate curve into a rMAR time series by normalizing the sedimentation rate curve by the whole-core mean sedimentation rate. We also extracted a PxI value for each annual layer by averaging the red, green, and blue pixel intensities using the boundaries calculated from semi-automated varve counting. Our objective in this study is to investigate the spectral properties of these cores' rMAR and PxI records, in order to evaluate possible paleo-climatic cyclicity in Southern Patagonia.

3.2. Core chronology and age-depth models

Lago Argentino's sediment is almost entirely composed of alternating light and dark laminae, interspersed with occasional event deposits. We investigated the source of these alternating light and dark laminae through a detailed sedimentary analysis, and showed that they are varves created by seasonal cycles in glacial sediment influx, fluvial sediment influx, and lake mixing (Van Wyk de Vries et al., 2022). We further cross-validated the annual nature of laminations at Lago Argentino through independent ^{137}Cs dating by comparing the varve count with the 1963–1965 ^{137}Cs peak (Van Wyk de Vries et al., 2022). We therefore use varve counting to build an age-depth model for each core based on the following findings: (i) there is a close match between varve count results and ^{137}Cs dating; (ii) multiple physical mechanisms exist at Lago Argentino that enable regular varve formation; (iii) grain size and sediment composition show consistent variations between light and dark lamina down the entire core depths; and (iv) the cores used in this study sample the ice-distal regions of Lago Argentino, where uninterrupted settling of fine sediment leads to a continuous sedimentary record.

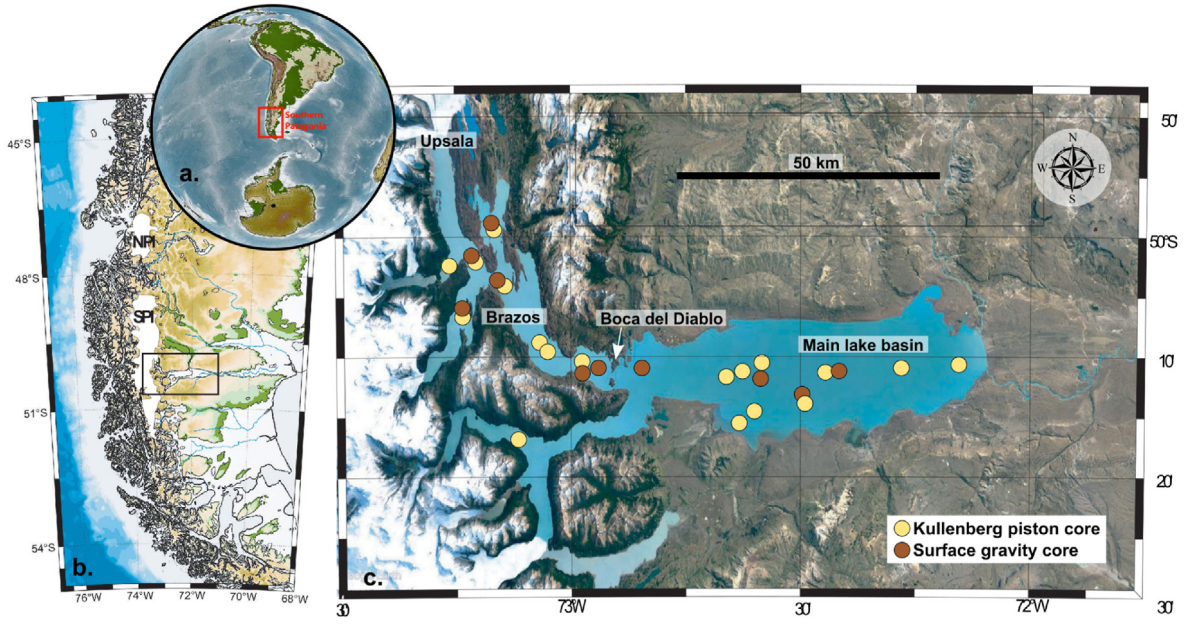

Fig. 1. Location of Lago Argentino and other key locations. The central globe (a) shows the location of Patagonia, and the left-hand panel (b) shows the location of Lago Argentino within Patagonia. The right-hand panel (c) shows the Lago Argentino basin and the position of the 28 cores used in this study.

We created an age-depth model for each core using sliding-window autocorrelation of greyscale digital core scans (CountMY-varves; see Van Wyk de Vries et al., 2021). This method uses sliding-window autocorrelation to identify repeated patterns in cores after manual identification and removal of event deposits and other non-varved sediment, such as damaged core tops. In addition to generating an age-depth model, the automated varve count provides a yearly resolution sedimentation rate curve for each core site. CountMYvarves evaluates the uncertainty in varve count by performing multiple counts on independent transects of the same digital core scan (Van Wyk de Vries et al., 2021), providing both a median age-depth model and likely bounds on the age for any given lamina.

Uncertainty in the age-depth model for each core results from two sources: uncertainty in the varve count itself, and uncertainty in the number of missing varves at the core top. The second term is zero where the sediment water interface is preserved, but this is seldom the case (particularly for Kullenberg piston cores). We determine likely bounds on the number of disrupted years at the core top from comparison between Kullenberg and gravity cores, and comparison between varve count and ^{137}Cs dates. We obtain the uncertainty in varve counting directly from CountMYVarves (Van Wyk de Vries et al., 2021). We then used Monte-Carlo sampling to generate an ensemble of 1000 age-depth models for each core, which we use in the following spectral analysis workflow. Median age-depth models, estimated uncertainty components, and Monte-Carlo ensemble age-depth models for each core are available in the supplementary materials.

3.3. Synthetic signal experiment

We designed an experiment to examine the effect of noise and signal corruption on the preservation of periodicity in sedimentary records. We created two annual-resolution synthetic climatic variable time series, each 1000 years long. One time series is composed of a single 100 year period sine wave, while the second is composed of the sum of a 100 year sine wave and a 25 year sine wave. We then constructed 24 synthetic proxy time series by modifying the time series of climatic variables in various ways. For example, the synthetic climatic variable could represent temperature and the synthetic proxy could represent sedimentation rate.

We divided the 24 synthetic proxy time series into three categories.

- Direct reproductions of the synthetic climatic variable with added noise. We created scenarios with 10, 50, and 200% white noise and red noise (Ghil et al., 2002), for signal to noise ratios of 10, 2, and 0.5 respectively. These scenarios represent the case where there is a direct, linear relationship between the synthetic climatic variable and synthetic proxy, but with the synthetic proxy incorporating additional noise.
- Time-averaged reproductions of the synthetic climatic variable with added noise. We smoothed the dataset using a 2, 10, and 50 year moving average and added 50% red noise (signal to noise ratio of 2) to the resulting signal. These scenarios represent the case where the synthetic proxy records a time-averaged version of the synthetic climatic variable. This might be the case in Lago Argentino, where sediment has a multiannual settling timescale (Van Wyk de Vries et al., 2022).
- Reproductions of the synthetic climatic variable without one or both of the assumptions necessary for proxy reconstruction: linearity and stationarity (National Research Council, 2006). We invalidated linearity through a quadratic relationship between the synthetic proxy and synthetic climatic variable, and stationarity by introducing a linear drift in the relationship between the synthetic proxy and synthetic climatic variable. We created three scenarios, one in which linearity is not met, one in which stationarity is not met, and one in which neither is met.

We analyzed the spectral properties of all synthetic proxy time series to identify whether or not periodicity is preserved through the various signal distortions. We computed a spectrogram for each of the 24 synthetic proxy time series using the multi-taper Lomb-Scargle periodogram (Springford et al., 2020) with the same algorithm as used for the Lago Argentino rMAR and PxI time series. We assessed the significance of spectral peaks against a first-order autoregressive red noise test (Ghil et al., 2002), and compared their magnitude to those of the synthetic climatic variable.

3.4. Spectral analysis of mass accumulation rate and pixel intensity time series

We carried out our spectral analysis through three primary steps, also shown in Fig. 2.

1) Manual pruning of outliers and normalization of time series. Monte-Carlo sampling of the uncertainty range.
2) Warping of individual core rMAR and PxI records to a common time axis via multivariate dynamic time warping
3) Conversion of rMAR and PxI to the spectral domain using the Multitaper Lomb-Scargle method, and extraction of significant periodicities.

We remove very-high rMAR outliers related to event deposits from the rMAR and PxI time series. rMAR in Lago Argentino varies an order of magnitude with distance from the glacier fronts, so we normalized each rMAR curve based on its mean rMAR in order to compare the temporal variations between different zones of Lago Argentino. For consistency, we also divided PxI time series by their averages, although mean PxI varies by less than a factor of two across Lago Argentino.

Disrupted sediment related to core extraction, sub-sectioning, and splitting introduces inevitable gaps in the rMAR and PxI record. Varve counting itself also leads to uncertainties into both the age-depth model and rMAR record, which complicates matching between individual sedimentation time series. PxI values were extracted using the same age-depth model, and so are sensitive to the same uncertainties. We generated composite rMAR records to create a continuous rMAR and PxI record for Lago Argentino and warp individual cores to a common time axis and reduce temporal uncertainty. We separated cores by depositional environments (brazos and main lake basin) and by coring mechanism (piston and gravity corer), for a total of 4 groups.

We generated 1000 rMAR and PxI curves for each individual core using the Monte-Carlo sampled age-depth models. We then used multivariate dynamic time warping to composite each of these 1000 records within each group. Dynamic time warping is widely used in paleo-climate research for aligning multiple proxies to a master curve, or to an external record of orbital forcing (Lisiecki and Lisiecki, 2002). In most cases, these algorithms work by warping one or multiple 'unknown' time series to match a 'reference' or 'master' time series. This approach is not suited for our case, however, as all rMAR and PxI time series we wish to composite are equally unknown, and no 'reference' time series exists. We instead used an alternative form of multivariate dynamic time warping, Fast Learnable Time Warping (FLTW, Khorram et al., 2019), which is designed for compositing multiple equally weighted time series. We modified Khorram et al. (2019)'s FLTW algorithm to work on unevenly sampled signals so as to exclude regions of missing sediment. We also lowpass filter signals prior to

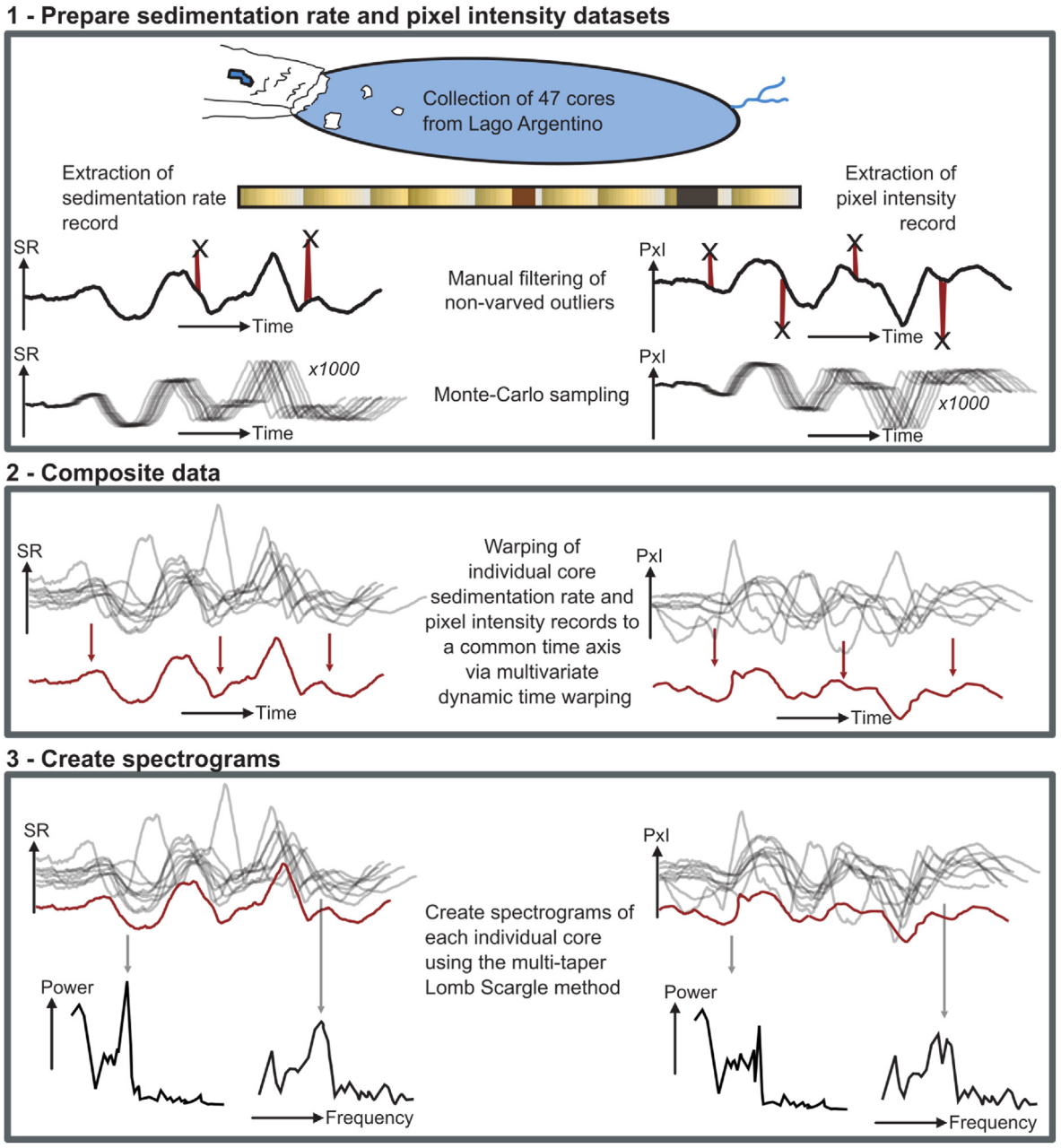

Fig. 2. Spectral analysis workflow.

matching to prevent warping to local minima, and limit the maximum and minimum degree of local warping (to between 0.5 and 2 times the prior value). Warping time series based on convolution with shifted triangular filters has the advantage of automatically producing a smooth and continuous warped time series, while the difference matrix approach can produce physically implausible step-shaped outputs.

FLTW produces composite rMAR and PxI time series derived from all cores in a given group, and a time-warped rMAR and PxI curve for each individual core. We next calculated spectrograms for all cores. Most standard spectral analysis methods require a continuous, uniformly sampled time series, and are thus not suited for use on our dataset due to portions of disrupted sediment. We therefore used the multi-taper Lomb-Scargle periodogram, which is applicable to unevenly sampled time series with missing data (Springford et al., 2020). This approach averages multiple spectrograms over the same time series, each multiplied with a different discrete prolate spheroidal sequence (DPSS) taper, reducing the noise level of the resulting spectrogram (Springford et al., 2020).

We calculated a median spectrogram for each core using the spectrograms for the 10% of runs (100) with the lowest FLTW warping cost functions, corresponding to the best cross-match between different cores. We evaluated each spectrogram against a first-order autoregressive red noise test (Ghil et al., 2002), with thresholds at the 95% and 99% confidence intervals. Finally, we manually examined each mean spectrogram and extracted the highest power peaks from each record.

4. Results

4.1. Synthetic signal experiment

We designed the synthetic spectral test to investigate whether periodicity may be preserved in a proxy record, even in the presence of very high noise levels, lack of linearity, or lack of stationarity. The 100 year cycles are significant at the 99% level in the Lomb-Scargle periodogram in all 24 cases. The shorter 25 year cycle is significant at the 99% level in all except one of the 12 cases. Peaks remain above the 99% significance level even for a signal to noise ratio of 0.5, and with the invalidation of both the assumption of linearity and stationarity. Operations which systematically affect the amplitude of the signal period, such as smoothing (reduction of the amplitude) and a non-linear relation between signal and climatic variable (reduction or amplification of the amplitude depending on the type of non-linearity) also affect the amplitude of associated spectral peaks.

The addition of 10–50% red or white noise to the synthetic proxy has a negligible effect on its spectrum. The addition of 200% red or white noise slightly affects the relative shape and magnitude of the spectral peaks, but both the 25 and 100 year period peaks remain highly significant and distinct from the background (Fig. 3). The long-term mean of the reconstructed synthetic proxy signal remains identical to the original synthetic climate signal for white noise and close for red noise, although the uncertainties associated with the reconstruction can be high (Fig. 3 f and h). In the case of 200% red noise addition, the magnitude and phase of the reconstructed periodicity varies considerably between cycles (Fig. 3 f and h). The addition of moderate amounts of noise to the synthetic proxy signal, in the absence of other changes, does not affect the preservation of spectral peaks.

Smoothing reduces the magnitude of the resulting synthetic proxy signal relative to the original synthetic climatic variable, and alters its phase. In the extreme case where the degree of smoothing is equal to or longer than a given cycle's periodicity, the cycle may be erased entirely (Fig. 4 h). Smoothing of the synthetic proxy over two years has little to no effect on the 25 or 100 year spectral peaks. Smoothing of the signal over 10 years also has little effect on the 100 year period spectral peak, but reduces the power of the 25 year spectral peak by half (Fig. 4 b and d). It also shifts the phase of both peaks by around 5 years. Smoothing of the signal over 50 years erases the 25 year cycle entirely, with the resulting double-period synthetic proxy reconstruction becoming near-identical to the single-period case (Fig. 4 h). The 25 year spectral peak is absent, and the power of the 100 year spectral peak is reduced by half. The phase of the 100 year signal is shifted by 25 years, or one quarter period.

A non-linear relationship between the synthetic climatic signal and synthetic proxy results in a distorted signal. For the quadratic

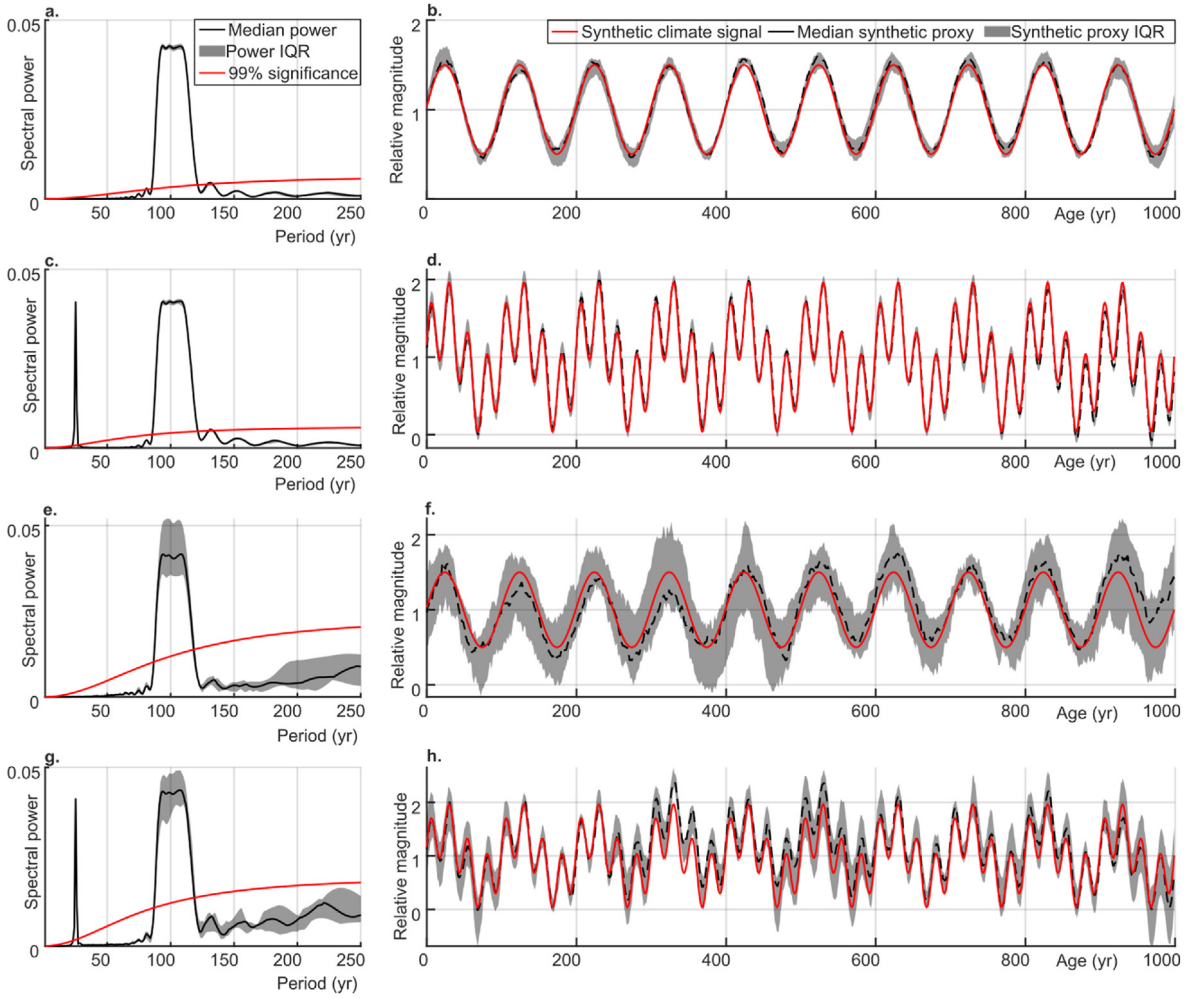

Fig. 3. Spectra (a, c, e, g) and synthetic climatic variable-proxy comparison (b, d, f, h) for the addition of 50% red noise (a–d) or 200% red noise (e–h). The resulting signal to noise ratio of the proxy is 2 (a–d) or 0.5 (e–h). IQR = Interquartile range.

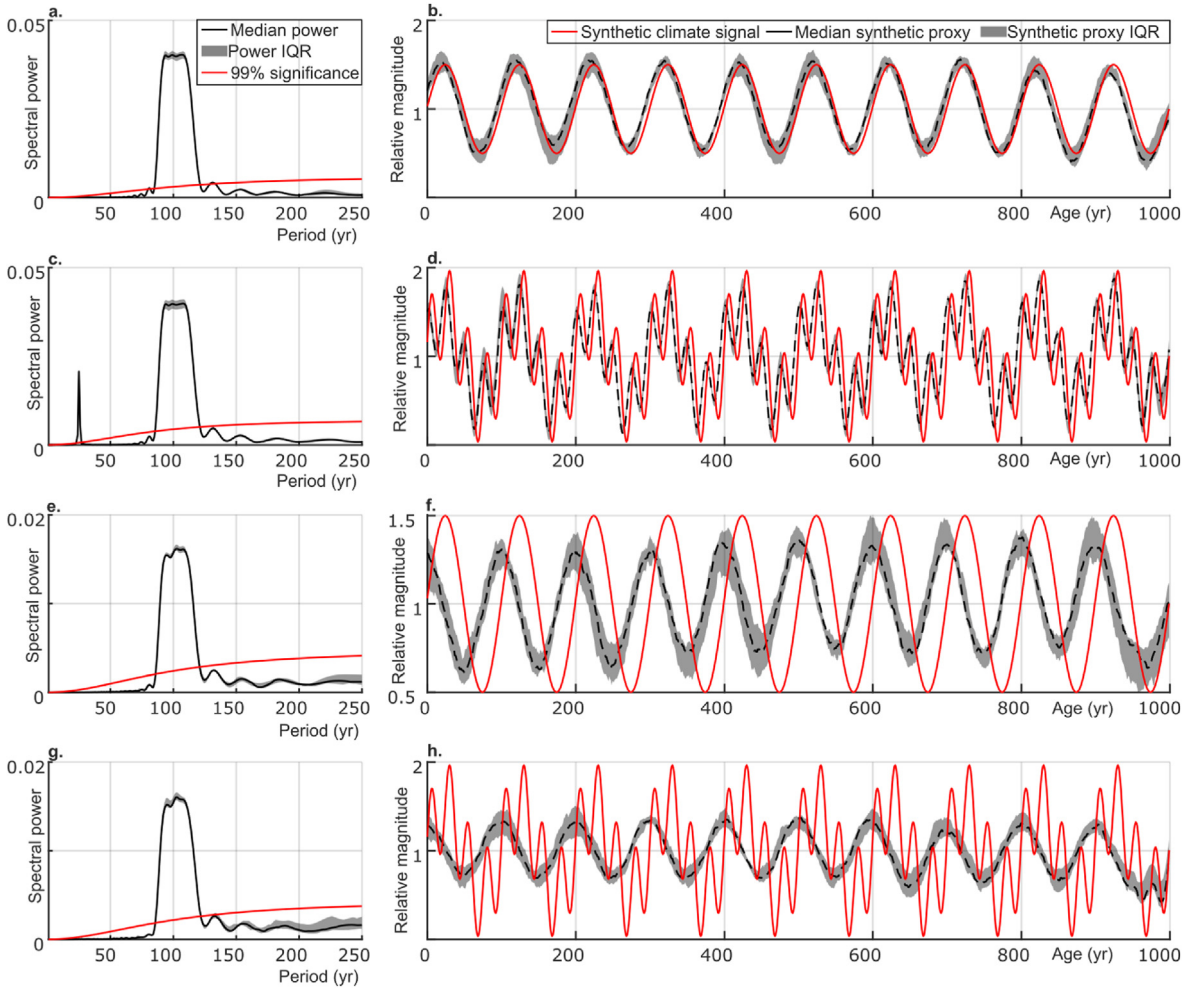

Fig. 4. Spectra (a, c, e, g) and synthetic climatic variable-proxy comparison (b, d, f, h) for 10 (a–d) and 50 (e–h) year smoothing of the signal.

signal-proxy relationship used here, the amplitude of the cycle is increased. This is particularly notable in the case with two superimposed period signals, as the amplitude of the shorter-period (25 yr) signal becomes modulated by the longer-period (100 yr) signal. The amplitude of the 25 year cycle is high when the 100 year cycle is close to its maxima, and low when the 100 year cycle is near its minima (Fig. 5 d). The power of the 25 year and 100 year spectral peaks is greater than for the original synthetic climate signal, but artifacts are also introduced into the signal (Fig. 5 a and c). The single-cycle case (100 year) has two additional peaks significant at the 99% level (81 and 132 years, Fig. 5 a), while the dual-cycle case (25 and 100 year) has three additional peaks significant at the 99% level (20, 34, and 132 years, Fig. 5 c). Non-linearity may therefore preserve or even enhance the spectral peaks relative to the original signal, but may also introduce apparently significant false spectral peaks as a result of changes to the signal shape.

A non-stationary relationship between the synthetic proxy and synthetic climatic variable has very little effect on the spectral properties of the signal. The position and magnitude of both the 100 year and 25 year peaks are largely unchanged relative to the case where the relationship between the synthetic proxy and synthetic climatic variable is stationary. The linear shift in the relationship between the synthetic proxy and synthetic climatic variable introduces errors into the proxy reconstruction, which grow larger through time (Fig. 5 f and h).

Our results highlight how modifications to the original climatic signal affect the spectra and proxy reconstruction in different ways (Fig. 6). The addition of noise increases the uncertainty of proxy reconstructions, but has little direct effect on their spectra. Smoothing modifies the magnitude and phase of proxy reconstructions, and reduces the power of spectral peaks. If the timescale of smoothing is equal or greater than the period of a cycle, the cycle is erased entirely as expected. Breakdown of the assumption of linearity results in a failure to accurately reconstruct the variance of the original climatic signal, while breakdown of the assumption of stationarity results in a failure to accurately reconstruct the magnitude of the original climatic signal. While these render records unsuitable for use as paleoclimatic proxies using standard techniques, they only have a minor effect on the spectral properties of signals. Therefore, the periodicity in the original climatic forcing may be recovered from sedimentary records even where they cannot be used to quantitatively reconstruct the original climatic forcing itself.

4.2. Spectral analysis of mass accumulation rate and pixel intensity time series

Composite dynamic-time-warping aligned time series show the variations in rMAR and PxI through time. All four groups, main basin piston (Kullenberg) cores, the brazos piston cores, the main basin gravity cores, and the brazos gravity cores, show a decreasing sedimentation trend over the past few decades. The two gravity

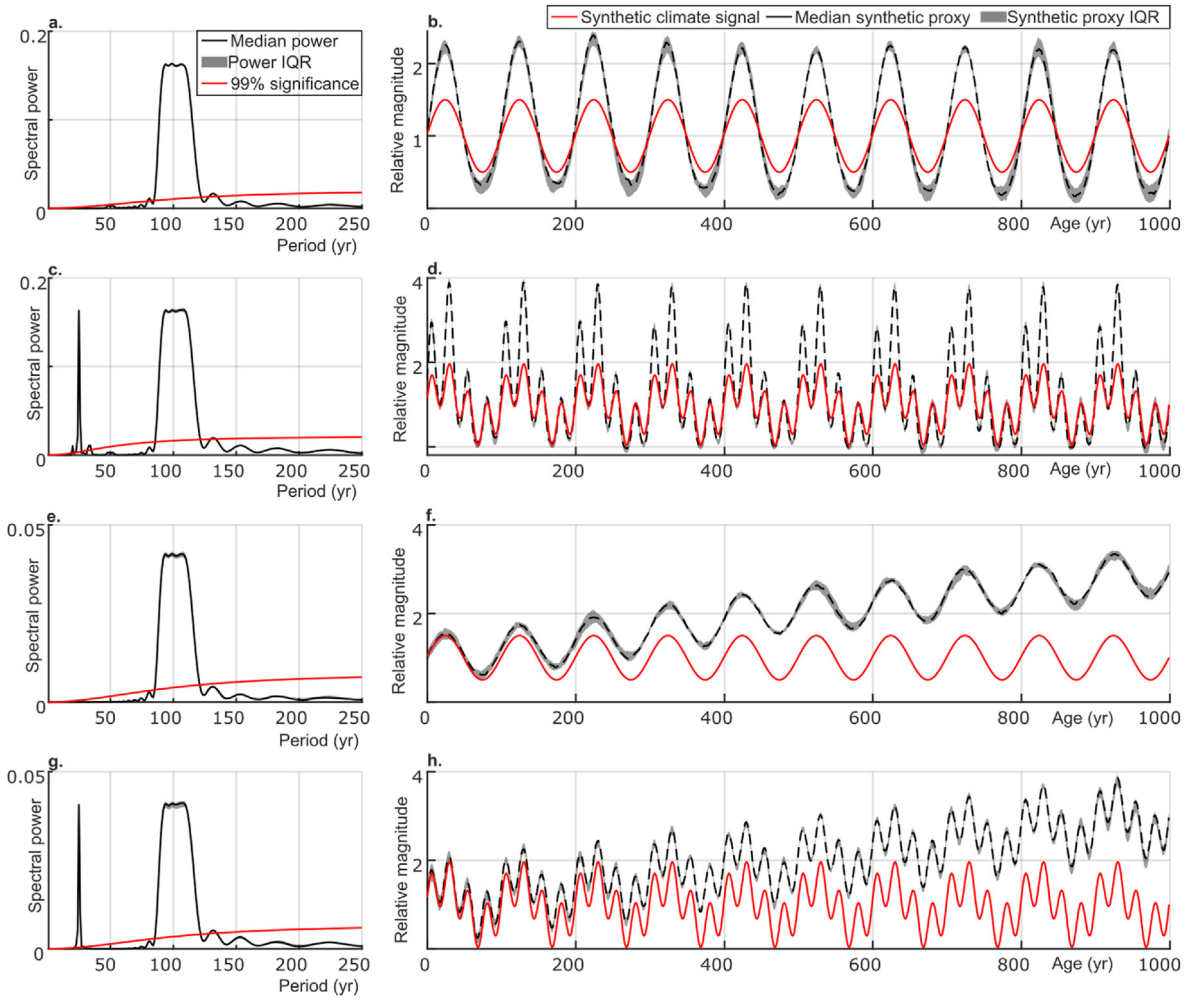

Fig. 5. Spectra (a, c, e, g) and synthetic climatic variable-proxy comparison (b, d, f, h) for a breakdown of the assumption of linearity (a–d) and a breakdown of the assumption of stationarity (e–h).

core groups do not exhibit any clear long-term trends, but extend at most 600 years. The two piston core groups are longer, with their records covering the past ~1800 years for the brazos and ~5000 years for the main basin. They both exhibit similar temporal patterns in sedimentation, with higher than average sedimentation over the past 300 years, 600–1000 years ago, and around 1500 years ago (Fig. 7). Correspondingly lower than average rMARs are found centered on 400 years ago and 1200 years ago in both records. rMAR at Lago Argentino has varied within ~25% of the present-day value over the past 5000 years.

Spectral analysis of individual core time series provides information about the dominant periodicities within their sedimentary record. Both the rMAR time series and PxI time series exhibit statistically significant peaks in their spectrograms, although these are more common for the rMAR data. The highest power peak in most piston core spectrograms has a very long period, between 300 and 2500 years. This peak does not exhibit any consistency in its period between different cores, varying across almost an order of magnitude. A number of other significant shorter period spectral power peaks are, however, found in multiple cores: one at 200 ± 20 year period, another at 150 ± 16 year period, and a third at 85 ± 9 year period (e.g., Fig. 8).

We first assess the presence and significance of the 200 ± 20, 150 ± 16, and 85 ± 9 year period spectral power peaks in the rMAR time series for all 28 cores. The 200 ± 20 year period spectral power peak is present and statistically significant at the 95% level in 61% of all cores (17), and in 78% of the longer Kullengerg piston cores (14 out of 18). The peak remains significant at the 99% level in 54% of all cores (15) and 67% of the piston cores (12). The 150 ± 16 year period spectral power peak is present and statistically significant in 57% of all cores (16), and in 78% of the longer Kullenberg piston cores (14). The peak remains significant at the 99% level in 54% of all cores (15) and 72% of the piston cores (13). The 85 ± 9 year period spectral power peak is present and statistically significant in 61% of all cores (17). The peak remains significant at the 99% level in 46% of all cores (13) and 60% of the surface gravity cores (6). A further 35 ± 4 year period spectral power peak is present and significant at the 95% level in 32% of all cores (9), but is only significant at the 99% level in 2 cores. The 200, 150, and 85 yr spectral power peaks are significant at the 99% level in the rMAR time series across much of Lago Argentino.

Next, we assess the presence and significance of the same 3 spectral power peaks in the PxI time series for all 28 cores. The 200 ± 20 year period spectral power peak is present and statistically significant in 36% of all cores (10), and in 67% of the brazos Kullenberg piston cores (6). The spectral power peak remains significant at the 99% level in 25% of all cores (7). The 150 ± 16 year period spectral power peak is present and statistically significant in 36% of all cores (10), and in 56% of the brazos Kullenberg piston

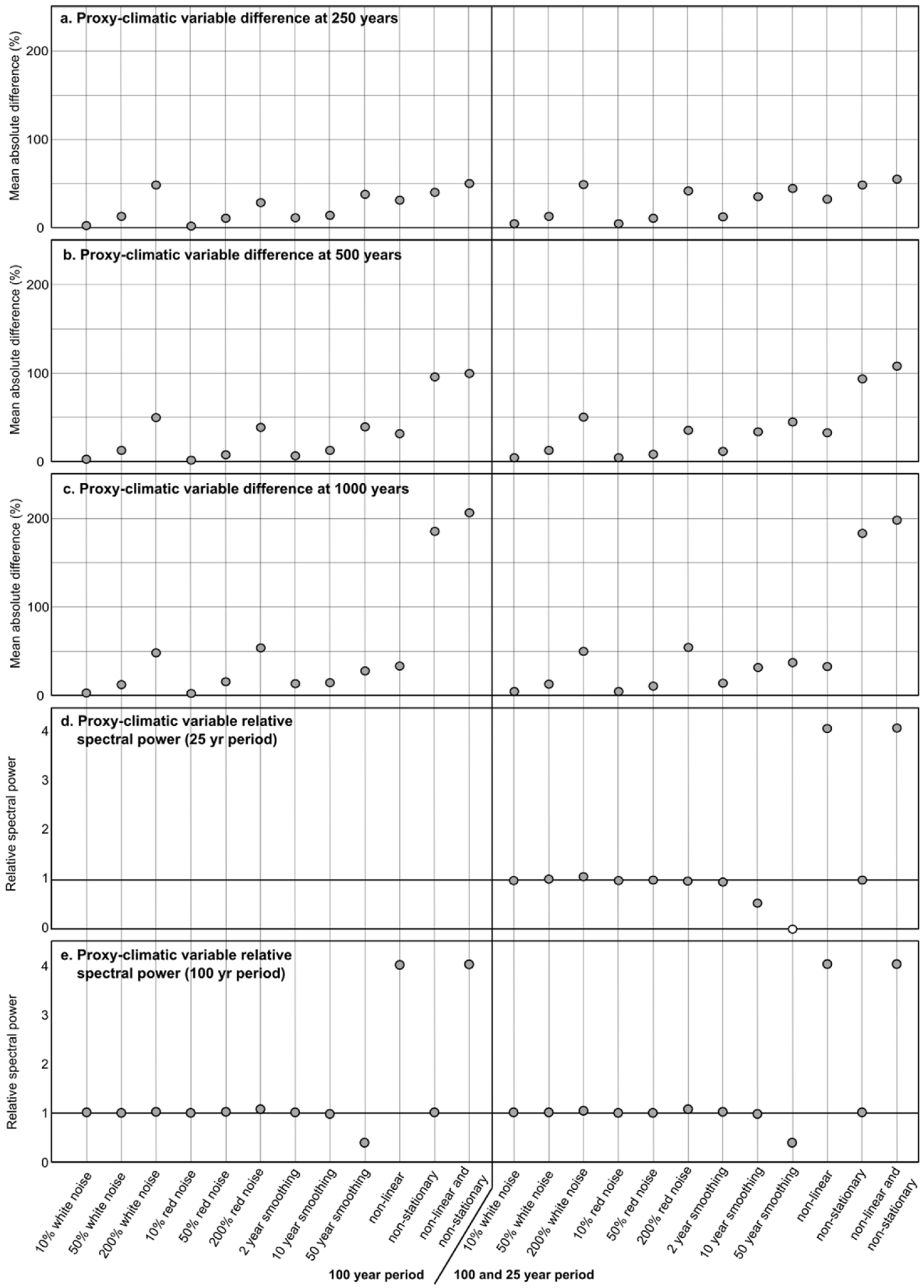

Fig. 6. Summary of the effect of noise addition, smoothing, non-linearity, or non-stationarity on the relative spectral power and mean absolute difference between the synthetic proxy and original synthetic climatic variable.

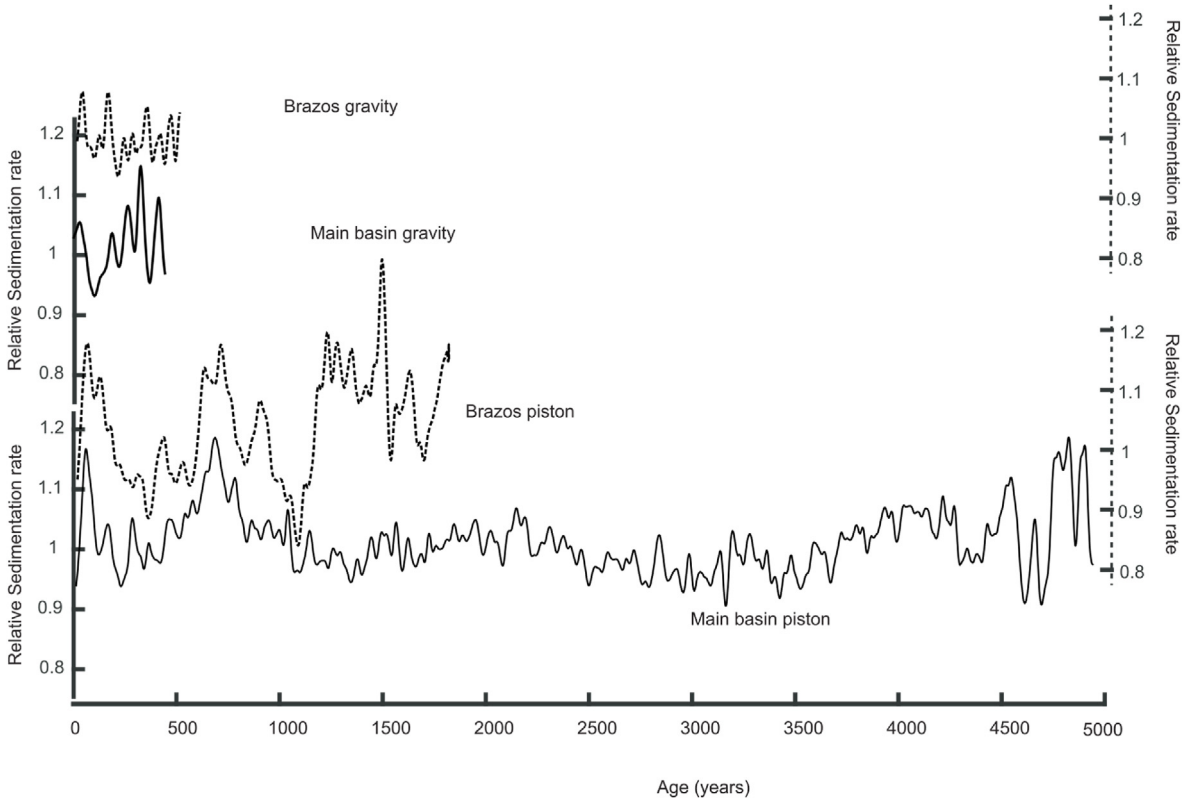

Fig. 7. Composite relative rMAR time series for the four groups investigated in this study: the main basin piston (Kullenberg) cores, the brazos piston cores, the main basin gravity cores, and the brazos gravity cores.

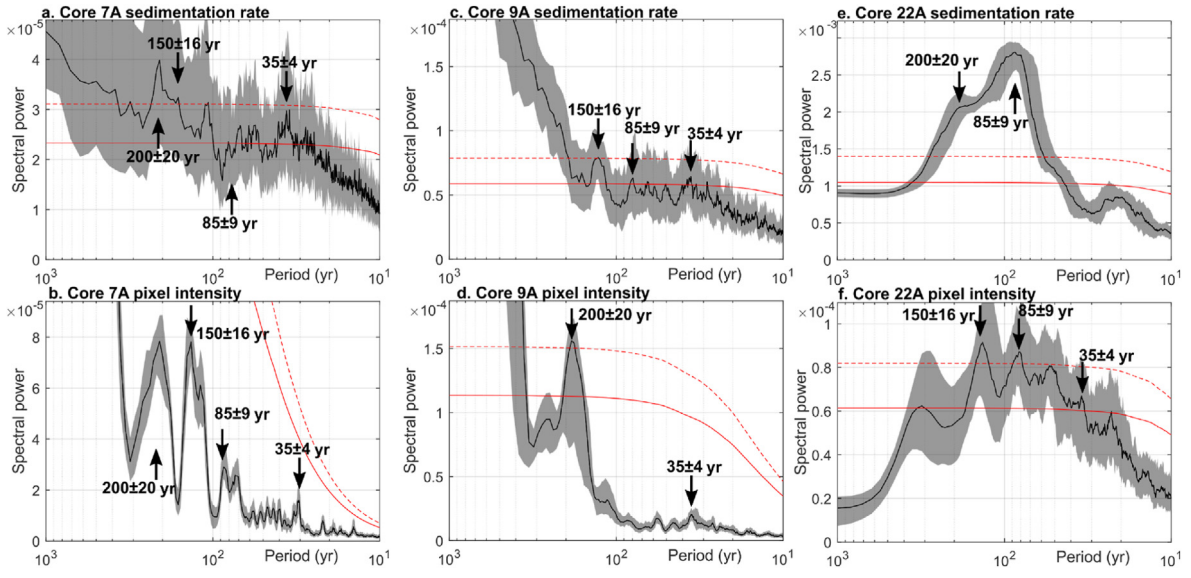

Fig. 8. Spectrograms for rMAR (a, c, e) and PxI (b, d, f) for piston cores 7A and 9A, and gravity core 22A.

cores (5). The peak remains significant at the 99% level in 29% of all cores (8). The 85 ± 9 year period spectral power peak is present and statistically significant in 18% of all cores (5), and in 67% of the brazos surface gravity cores (4). The peak remains significant at the 99% level in 14% of all cores (4). The three PxI spectral power peaks are present in fewer cores than for the rMAR time series, but are still present in all Lago Argentino's main depositional environments.

5. Discussion

Our synthetic proxy test shows that periodicity is commonly preserved even in very noisy or otherwise poorly preserved proxy records. Three assumptions are necessary in order to use a dataset as a paleoclimate proxy using the standard linear regression approach: the relationship between the proxy and climatic variable of interest must be linear (National Research Council, 2006), the

statistical relationship between a given proxy and a given climatic variable must remain constant throughout the entire study period (National Research Council, 2006), and the noise level in the proxy record must be low enough to not overwhelm the climatic signal. These assumptions are commonly not met in natural systems. A possible proxy record may be affected to a different extent by different climatic variables through time: for example, a tree's growth may be temperature-limited in some years and precipitation-limited in others. Failure of these assumptions for any proxy precludes quantitative reconstruction of the magnitude of past climate. Our synthetic test results, however, show that it does not prevent the reconstruction of the spectral properties of climatic signals. Lago Argentino exhibits a complex sedimentary environment with multiple competing climatic controls on sedimentation (Van Wyk de Vries et al., 2022), such as temperature (glacier melt) and wind speed (lake mixing), and a high likelihood that the relationship between sediment deposition and climate is not stationary at any given location. Therefore, we examine the spectral properties of Lago Argentino's sediment with the objective of recovering any dominant periodicities in the climatic drivers of sedimentation.

We identify three main statistically significant periodicities through spectral analysis of Lago Argentino's sedimentary record: 200 ± 20, 150 ± 16, and 85 ± 9 years. We investigate the spectral properties of 28 individual cores, and find that these three periods remain significant across all of Lago Argentino's main depositional environments. In addition, these three periods (200 ± 20, 150 ± 16, and 85 ± 9 years) are statistically significant in both of the different sedimentary proxies which we use: rMAR and PxI. The peaks are present most widely in the rMAR spectra (57–64% of all cores, ~three quarters of piston cores. The longer period peaks (200 ± 20 and 150 ± 16 years) are most commonly found in the piston core spectra covering longer timescales, while the shorter period peak (85 ± 9 years) is most commonly found in the surface gravity cores with shorter records. Other periodicities are statistically significant in some cores, including very long periods (300–2500 years) and shorter periods (35 ± 4 years), although they are only significant across a small fraction of our dataset. The lower abundance of significant 200 ± 20 and 150 ± 16 year peaks in the gravity cores is unsurprising, given that many gravity cores record fewer than one period of data. The ability of gravity cores to resolve the recent past, along with their high number of significant 85 ± 9 year spectral peaks, means they remain useful to include in this study. The commonality of periodicities across Lago Argentino's basin leads us to relate them to large-scale climatic forcings.

Detailed analysis of Lago Argentino's sedimentary record (Van Wyk de Vries et al., 2022, 2021) and investigation of present-day climate and lacustrine processes in the area (Garreaud et al., 2012; Richter et al., 2016; Sugiyama et al., 2016) provides insight into the likely climatic controls on sediment deposition at Lago Argentino. Sediment in Lago Argentino is primarily sourced from glacial erosion, with a minor fluvial contribution (Van Wyk de Vries et al., 2022). The timescales of sediment deposition are also affected by the degree of lacustrine stratification, which is controlled by a balance between wind-derived kinetic energy and thermal-stratification-derived potential energy (Fischer et al., 1979; Van Wyk de Vries et al., 2022). The timescales of Stokes' settling for the micron-scale grain fraction which constitutes the majority of Lago Argentino's sediment may be as high as several decades (Van Wyk de Vries et al., 2022), but remains shorter than even the shortest significant periodicity we identify (85 ± 9 years) in both the fully mixed and fully stratified endmember cases. Consequently, the rate of glacial erosion is likely the major control on sedimentation in Lago Argentino on centennial timescales.

The total volume of sediment eroded by a glacier over a given time period is controlled by two factors: the size of the glacier, and its area-integrated erosion rate. As a glacier grows, it is in contact with the bed over a larger area, and all else being equal, will erode a larger volume of sediment. Glacier erosion rate at any point in space is, on a first order, controlled by glacier sliding speed (Cook et al., 2020). The deposition of glacially eroded sediment also diminishes away from the glacier front. This reduction in sedimentation rate with distance has been approximated by either a single or dual exponential decay function (Koppes and Hallet, 2002). The accumulation rate of glacially-derived sediment at a given point in a proglacial lake basin is therefore sensitive to three factors: the total size of the contributing glacier, the sliding speed of this glacier, and the distance between the point and the glacier's calving front. Glaciers will generally grow when climatic variables positively influence their surface mass balance with a decrease in temperature or an increase in precipitation (Cuffey and Paterson, 2010; Hock, 2005). Positive SAM phases are associated with warming and drying across the Lago Argentino glacier catchment area, which is located on the leeward side of the Andean cordillera (Garreaud et al., 2009; Reynhout et al., 2019). Conversely, negative SAM phases are associated with cooling and increases in precipitation. Both the precipitation and temperature effects of the SAM have complementary effects on glacier mass balance, promoting growth during SAM-negative phases and recession during SAM-positive phases (e.g., Reynhout et al., 2019). The coupled temperature and precipitation effects of the SAM, driving periods of positive and negative glacier mass balance, thus are a likely driver of centennial scale variations in sediment properties at Lago Argentino.

While the SAM provides a plausible mechanism for centennial scale sediment variability at Lago Argentino, other factors may also influence sedimentation. Both lakes and glaciers may exhibit non-climatically forced periodic or quasi-periodic fluctuations. Richter et al. (2016) identified a periodic seiche current in Lago Argentino using pressure tide gauges with a dominant period of 85 min and secondary periodicities of 28–107 min, but no study has indicated the presence of multidecadal internal lake periodicities. Glaciers may exhibit two main types of internal variability: surges (Sevestre and Benn, 2015) and the tidewater glacier cycle (Cuffey and Paterson, 2010). Glacier surges have not been observed in Patagonia, with the possible exception of the multidecadal advance of Glaciar Pio XI (Rivera and Casassa, 1999; Hata and Sugiyama, 2021). A global survey of the conditions conducive to glacier surging suggests that they are unfavorable in Patagonia due to the warm temperatures (Sevestre and Benn, 2015). Non-linear retreat has also been observed at Glaciar Upsala, the largest glacier in the Lago Argentino catchment, but this has not been associated with a tidewater cycle (Sakakibara et al., 2013). Glaciar Upsala's hypsometry is similar to that of Glaciar San Rafael, where Warren (1993) concluded that climate remained the primary driver of glacier retreat over multidecadal timescales. Glacier surges are thus unlikely at Lago Argentino, and any tidewater glacier processes may distort any climatic signal but not overprint it with a non-climatic periodicity. Overall, multidecadal to centennial internal periodicities in Lago Argentino's glacio-lacustrine system are not likely, and any such periodicity preserved in the sedimentary record reflects periodicity in the climatic forcing.

On the balance of evidence, the SAM is the most likely cause for the statistically significant 200 ± 20, 150 ± 16, and 85 ± 9 year periodicities in Lago Argentino. This is consistent with Moreno et al. (2014)'s findings which ascribe 200 ± 60 year long positive non-arboreal pollen anomalies to positive SAM phases in Lago Cipreses, 100 km south of Lago Argentino, and with Reynhout et al. (2019)'s posit that the SAM has paced glacier advances and retreats across Patagonia. As our study only evaluates periodicities over the entire core lengths, we cannot confirm Villalba et al.

(2012)'s finding of an unusual SAM behaviour over the late 20th century. However, our study provides valuable information about the baseline state of the SAM in Southern Patagonia. Our study does not attempt to correlate specific SAM-positive or SAM-negative phases to episodes of glacier advance and retreat, but instead provides a broader context for the understanding of their periodic climatic drivers. The three spectral peaks are less common in the PxI record than rMAR, which suggests that the processes affecting sediment accumulation rate in Lago Argentino are more closely coupled to larger-scale climate drivers than those controlling sediment color. Detailed investigation of the present-day physical processes operating in Lago Argentino may provide insight into the exact source of these differences.

These multidecadal to centennial SAM periodicities have not been previously identified in Patagonia. We consider three reasons why the three 200 ± 20, 150 ± 16, and 85 ± 9 year periodicities are found for the first time in this study.

i) Only a very small number of prior studies have both an annual resolution and millennial temporal extent. Most annual resolution tree-ring studies extend only a few centuries into the past (Villalba et al., 2012), while most longer records have coarse temporal resolutions unsuited for the spectral identification of 85–200 yr periodicities (Caniupán et al., 2014; Massaferro and Larocque-Tobler, 2013).
ii) Lago Argentino's geographic location and sedimentary properties are ideally suited for recording changes in the SAM and SWW. With a glacierized basin at a latitude of 50°S, close to the core of the SWW wind belt, Lago Argentino is sensitive to the temperature and precipitation changes associated with positive and negative SAM phases (Garreaud et al., 2012; Kaplan et al., 2016). Lago Argentino directly preserves changes in glacial sediment yield with no modification from an intermediary fluvial system (Van Wyk de Vries et al., 2022), as is the case with non ice-contact lakes (Elbert et al., 2015, 2012). The presence of varves preserves annual resolution sediment properties and allows for the construction of a high resolution age-depth model.
iii) The methods applied in this study are well suited for the identification of a significant periodicity in noisy data. Firstly, we take care to use not a single record from Lago Argentino, but all 28 suitable sediment cores. Secondly, we make use of these multiple cores to create a composite time axis and age-depth model, with greater confidence than for any individual core. Finally, our choice of spectral analysis method, the multitaper Lomb-Scargle periodogram (Springford et al., 2020), is ideal for the recovery of weak periodicities in noisy and unevenly sampled data.

Similarly to how the eccentricity, obliquity, and precession of the Earth interfere to form a complex climatic signal, the 200 ± 20, 150 ± 16, and 85 ± 9 year SAM periodicities can constructively and destructively interfere to create irregularly spaced episodes of strongly positive or negative glacier forcing (Fig. 9). This may result in brief periods of extremely positive or strongly negative glacier mass balance for Patagonian glaciers. Today, Patagonian glaciers are rapidly losing mass (Abdel Jaber et al., 2019), with some estimates placing their specific mass change rate as the most rapid on Earth (Zemp et al., 2019). Assessments of future Patagonian ice loss forecast that this rapid ice loss is likely to be maintained or even accelerate in coming decades (Bravo et al., 2021). These studies do not, however, account for possible SAM periodicity. If the current negative glacier surface mass balance is amplified by the positive SAM phase (Aravena and Luckman, 2009; Garreaud et al., 2012), then a switch to a negative SAM phase may mitigate glacier mass loss. This attenuating factor is, however, conditioned upon the SAM

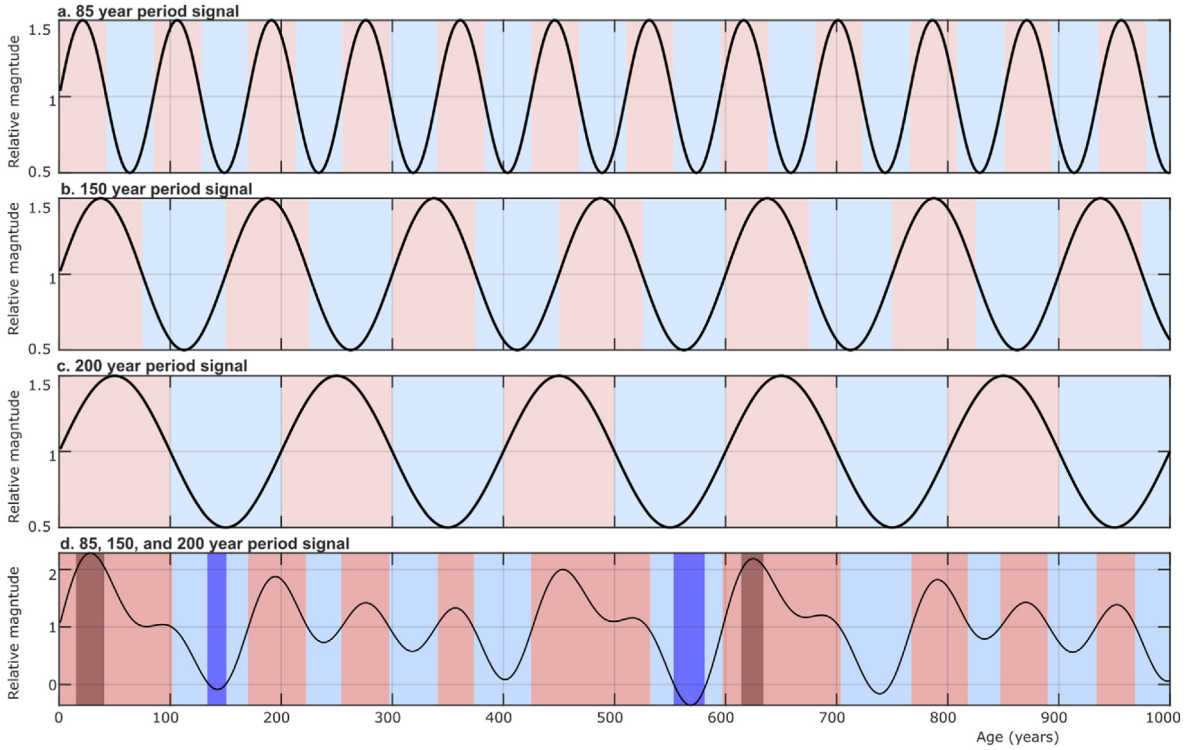

Fig. 9. 85, 150, and 200 year signals and their cumulative summed signal. The resulting signal exhibits periods of unusually high (indicated by dark red bars) and low (indicated by dark blue bars) magnitude, exceeding the amplitude of any of the individual cycles.

retaining its past periodic behavior into the future, which is uncertain due to strong anthropogenic atmospheric forcing (Villalba et al., 2012; Abram et al., 2014; Fogt and Marshall, 2020).

6. Conclusions

We use the sedimentary record of a large lake, Lago Argentino, to investigate the climatic drivers of sedimentation in Southern Patagonia. Our key findings are as follows.

1. Tests using a synthetic climate and proxy signal show that periodicity may be preserved even in cases where the proxy record is not suitable for paleoclimate reconstruction.
2. Spectral analysis of the rMAR and PxI record from 28 cores covering all of Lago Argentino's main depositional environments reveals three statistically significant periodicities: 200 ± 20, 150 ± 16, and 85 ± 9 years.
3. We relate the three significant multidecadal to centennial periodicities to variations in the SAM and associated changes in precipitation and temperature. Our results support the hypothesis that positive SAM phases promote glacier recession and negative SAM phases promote glacier advance.

Credit author statement

Maximillian Van Wyk de Vries: Conceptualization, Methodology/Study design, Software, Validation, Formal analysis, Investigation, Resources, Data curation, Writing – original draft, Writing – review and editing, Visualization, Funding acquisition. Emi Ito: Conceptualization, Methodology/Study design, Validation, Formal analysis, Investigation, Resources, Data curation, Writing – review and editing, Supervision, Project administration, Funding acquisition. Matias Romero: Conceptualization, Methodology/Study design, Validation, Formal analysis, Investigation, Resources, Data curation, Writing – review and editing. Mark Shapley: Conceptualization, Methodology/Study design, Validation, Formal analysis, Investigation, Resources, Data curation, Writing – review and editing, Supervision, Project administration. Guido Brignone: Conceptualization, Methodology/Study design, Validation, Formal analysis, Investigation.

Declaration of competing interest

The authors declare that they have no known competing financial interests or personal relationships that could have appeared to influence the work reported in this paper.

Data availability

All data used in this study is available online as linked to in the paper.

Acknowledgements

MV was supported by a University of Minnesota College of Science and Engineering Fellowship and a Doctoral Dissertation Fellowship. We acknowledge the critical role played by logistical and design expertise of Ryan O'Grady and Anders Noren of the CSD Facility in planning and field phases of this research. Kristina Brady Shannon, Jessica Heck, Alex Stone and Rob Brown seamlessly coordinated core processing and analytical activities at the CSD Facility. We thank Anastasia Fedotova, Cristina San Martín, Guillermo Tamburini-Beliveau, Alexander Schmies and Shanti Penprase for their help with core recovery and processing, and all Spanish-speaking team members for their critical contribution of language skills. We further thank editor Claudio Latorre and an anonymous reviewer for their valuable comments. This material is based upon work supported by the National Science Foundation under Grant No. EAR-1714614, coordinated by Lead PI Maria Beatrice Magnani. Data on the Lago Argentino cores are available from the CSD Facility at https://cse.umn.edu/csd/projects. Full resolution core scans and stratigraphic information are available at 10.5281/zenodo.5815107. The code used to count laminations in the cores, countMYvarves, is freely available under a GPL3.0 license at doi.org/10.5281/zenodo.4031812.

Appendix A. Supplementary data

Supplementary data to this article can be found online at https://doi.org/10.1016/j.quascirev.2023.108009.

References

Abdel Jaber, W., Rott, H., Floricioiu, D., Wuite, J., Miranda, N., 2019. Heterogeneous spatial and temporal pattern of surface elevation change and mass balance of the Patagonian ice fields between 2000 and 2016. Cryosphere 13, 2511–2535. https://doi.org/10.5194/tc-13-2511-2019.

Abram, N.J., Mulvaney, R., Vimeux, F., Phipps, S.J., Turner, J., England, M.H., 2014. Evolution of the southern annular mode during the past millennium. Nat. Clim. Change 4, 564–569. https://doi.org/10.1038/nclimate2235.

Aravena, J.-C., Luckman, B.H., 2009. Spatio-temporal rainfall patterns in southern south America. Int. J. Climatol. 29, 2106–2120. https://doi.org/10.1002/joc.1761.

Bravo, C., Bozkurt, D., Ross, A.N., Quincey, D.J., 2021. Projected increases in surface melt and ice loss for the Northern and Southern Patagonian Icefields. Sci. Rep. 11, 16847. https://doi.org/10.1038/s41598-021-95725-w.

Caniupán, M., Lamy, F., Lange, C.B., Kaiser, J., Kilian, R., Arz, H.W., León, T., Mollenhauer, G., Sandoval, S., De Pol-Holz, R., Pantoja, S., Wellner, J., Tiedemann, R., 2014. Holocene sea-surface temperature variability in the Chilean fjord region. Quat. Res. 82, 342–353. https://doi.org/10.1016/j.yqres.2014.07.009.

Cook, S.J., Swift, D.A., Kirkbride, M.P., Knight, P.G., Waller, R.I., 2020. The empirical basis for modelling glacial erosion rates. Nat. Commun. 11, 759. https://doi.org/10.1038/s41467-020-14583-8.

Cuffey, K.M., Paterson, W.S.B., 2010. The Physics of Glaciers. Academic Press.

Davies, B.J., Darvill, C.M., Lovell, H., Bendle, J.M., Dowdeswell, J.A., Fabel, D., García, J.-L., Geiger, A., Glasser, N.F., Gheorghiu, D.M., Harrison, S., Hein, A.S., Kaplan, M.R., Martin, J.R.V., Mendelova, M., Palmer, A., Pelto, M., Rodés, Á., Sagredo, E.A., Smedley, R., Smellie, J.L., Thorndycraft, V.R., 2020. The evolution of the Patagonian Ice Sheet from 35 ka to the present day (PATICE). Earth Sci. Rev., 103152 https://doi.org/10.1016/j.earscirev.2020.103152.

Davis, M.B., 1969. Palynology and environmental history during the Quaternary period. Am. Sci. 57, 317–332.

Elbert, J., Grosjean, M., von Gunten, L., Urrutia, R., Fischer, D., Wartenburger, R., Ariztegui, D., Fujak, M., Hamann, Y., 2012. Quantitative high-resolution winter (JJA) precipitation reconstruction from varved sediments of Lago Plomo 47 S, Patagonian Andes, AD 1530–2002. Holocene 22, 465–474.

Elbert, J., Jacques-Coper, M., Van Daele, M., Urrutia, R., Grosjean, M., 2015. A 600 years warm-season temperature record from varved sediments of Lago Plomo, Northern Patagonia, Chile (47°S). Quat. Int., Quat. Res. Across Americas 377, 28–37. https://doi.org/10.1016/j.quaint.2015.01.004.

Fischer, H.B., List, J.E., Koh, C.R., Imberger, J., Brooks, N.H., 1979. Mixing in Inland and Coastal Waters. Academic press.

Fogt, R.L., Marshall, G.J., 2020. The southern annular mode: variability, trends, and climate impacts across the southern Hemisphere. WIREs Clim. Change 11, e652. https://doi.org/10.1002/wcc.652.

Garreaud, R., Lopez, P., Minvielle, M., Rojas, M., 2012. Large-scale control on the patagonian climate. J. Clim. 26, 215–230. https://doi.org/10.1175/JCLI-D-12-00001.1.

Garreaud, R.D., Vuille, M., Compagnucci, R., Marengo, J., 2009. Present-day South American Climate. Palaeogeography, Palaeoclimatology, Palaeoecology, Long-Term Multi-Proxy Climate Reconstructions and Dynamics in South America (LOTRED-SA): State of the Art and Perspectives 281, pp. 180–195. https://doi.org/10.1016/j.palaeo.2007.10.032.

Ghil, M., Allen, M.R., Dettinger, M.D., Ide, K., Kondrashov, D., Mann, M.E., Robertson, A.W., Saunders, A., Tian, Y., Varadi, F., Yiou, P., 2002. Advanced spectral methods for climatic time series. Rev. Geophys. 40. https://doi.org/10.1029/2000RG000092.

Hata, S., Sugiyama, S., 2021. Changes in the ice-front position and surface elevation of glaciar pío XI, an advancing calving glacier in the southern Patagonia Icefield, from 2000–2018. Front. Earth Sci. 8, 681. https://doi.org/10.3389/feart.2020.576044.

Hauck, J., Völker, C., Wang, T., Hoppema, M., Losch, M., Wolf-Gladrow, D.A., 2013. Seasonally different carbon flux changes in the Southern Ocean in response to

the southern annular mode. Global Biogeochem. Cycles 27, 1236–1245. https://doi.org/10.1002/2013GB004600.
Hessl, A., Allen, K.J., Vance, T., Abram, N.J., Saunders, K.M., 2017. Reconstructions of the southern annular mode (SAM) during the last millennium. Prog. Phys. Geogr.: Earth Environ. 41, 834–849. https://doi.org/10.1177/0309133317743165.
Hock, R., 2005. Glacier melt: a review of processes and their modelling. Prog. Phys. Geogr.: Earth Environ. 29, 362–391. https://doi.org/10.1191/0309133305pp453ra.
Kaplan, M.R., Schaefer, J.M., Strelin, J.A., Denton, G.H., Anderson, R.F., Vandergoes, M.J., Finkel, R.C., Schwartz, R., Travis, S.G., Garcia, J.L., Martini, M.A., Nielsen, S.H.H., 2016. Patagonian and southern south atlantic view of Holocene climate. Quat. Sci. Rev. 141, 112–125. https://doi.org/10.1016/j.quascirev.2016.03.014.
Khorram, S., McInnis, M.G., Mower Provost, E., 2019. Trainable time warping: aligning time-series in the continuous-time domain. In: ICASSP 2019 - 2019 IEEE International Conference on Acoustics, Speech and Signal Processing (ICASSP). Presented at the ICASSP 2019 - 2019 IEEE International Conference on Acoustics. Speech and Signal Processing (ICASSP), pp. 3502–3506. https://doi.org/10.1109/ICASSP.2019.8682322.
Koppes, M.N., Hallet, B., 2002. Influence of rapid glacial retreat on the rate of erosion by tidewater glaciers. Geology 30, 47–50.
Lamy, F., Hebbeln, D., Röhl, U., Wefer, G., 2001. Holocene rainfall variability in southern Chile: a marine record of latitudinal shifts of the Southern Westerlies. Earth Planet Sci. Lett. 185, 369–382. https://doi.org/10.1016/S0012-821X(00)00381-2.
Lara, A., Villalba, R., Urrutia-Jalabert, R., González-Reyes, A., Aravena, J.C., Luckman, B.H., Cuq, E., Rodríguez, C., Wolodarsky-Franke, A., 2020. +A 5680-year tree-ring temperature record for southern South America. Quat. Sci. Rev. 228, 106087. https://doi.org/10.1016/j.quascirev.2019.106087.
Leger, T.P.M., Hein, A.S., Goldberg, D., Schimmelpfennig, I., Van Wyk de Vries, M.S., Bingham, R.G., , ASTER Team, Aumaitre, G., 2021. Northeastern patagonian glacier advances (43°S) reflect northward migration of the southern westerlies towards the end of the last glaciation. Front. Earth Sci. 9.
Lisiecki, L.E., Lisiecki, P.A., 2002. Application of dynamic programming to the correlation of paleoclimate records. Paleoceanography 17, 1. https://doi.org/10.1029/2001PA000733.
Marshall, G.J., 2003. Trends in the southern annular mode from observations and reanalyses. J. Clim. 16, 4134–4143. https://doi.org/10.1175/1520-0442(2003)016<4134:TITSAM>2.0.CO.
Marshall, G.J., Orr, A., Lipzig, N.P.M. van, King, J.C., 2006. The impact of a changing southern Hemisphere annular mode on antarctic peninsula summer temperatures. J. Clim. 19, 5388–5404. https://doi.org/10.1175/JCLI3844.1.
Massaferro, J., Larocque-Tobler, I., 2013. Using a newly developed chironomid transfer function for reconstructing mean annual air temperature at Lake Potrok Aike, Patagonia, Argentina. Ecol. Indicat. 24, 201–210. https://doi.org/10.1016/j.ecolind.2012.06.017.
Moreno, P.I., Vilanova, I., Villa-Martínez, R., Garreaud, R.D., Rojas, M., De Pol-Holz, R., 2014. Southern Annular Mode-like changes in southwestern Patagonia at centennial timescales over the last three millennia. Nat. Commun. 5, 4375. https://doi.org/10.1038/ncomms5375.
National Research Council, 2006. Surface Temperature Reconstructions for the Last 2,000 Years. The National Academies Press, Washington, DC. https://doi.org/10.17226/11676.
Neukom, R., Gergis, J., 2012. Southern Hemisphere high-resolution palaeoclimate records of the last 2000 years. Holocene 22, 501–524. https://doi.org/10.1177/0959683611427335.
Perren, B.B., Hodgson, D.A., Roberts, S.J., Sime, L., Van Nieuwenhuyze, W., Verleyen, E., Vyverman, W., 2020. Southward migration of the Southern Hemisphere westerly winds corresponds with warming climate over centennial timescales. Commun Earth Environ 1, 1–8. https://doi.org/10.1038/s43247-020-00059-6.
Reynhout, S.A., Sagredo, E.A., Kaplan, M.R., Aravena, J.C., Martini, M.A., Moreno, P.I., Rojas, M., Schwartz, R., Schaefer, J.M., 2019. Holocene glacier fluctuations in Patagonia are modulated by summer insolation intensity and paced by Southern Annular Mode-like variability. Quat. Sci. Rev. 220, 178–187. https://doi.org/10.1016/j.quascirev.2019.05.029.
Richter, A.J., Marderwald, E.R., Hormaechea, J.L., Mendoza, L.P.O., Perdomo, R.A., Connon, G.C., Scheinert, M., Horwath, M., Dietrich, R., 2016. Lake-Level Variations and Tides in Lago Argentino, Patagonia: Insights from Pressure Tide Gauge Records.
Rivera, A., Casassa, G., 1999. Volume changes on Pio XI glacier, Patagonia: 1975–1995. Global Planet. Change 22, 233–244. https://doi.org/10.1016/S0921-8181(99)00040-5.
Sakakibara, D., Sugiyama, S., Sawagaki, T., Marinsek, S., Skvarca, P., 2013. Rapid retreat, acceleration and thinning of glaciar Upsala, southern Patagonia Icefield, initiated in 2008. Ann. Glaciol. 54, 131–138. https://doi.org/10.3189/2013AoG63A236.
Saunders, A.H., Allen, Kathryn J., Vance, Tessa, Abram, Nerilie J., Krystyna, M., 2017. Reconstructions of the southern annular mode (SAM) during the last millennium. In: Hessl, Amy, Allen, Kathryn J., Vance, Tessa, Abram, Nerilie J., Saunders, Krystyna M. (Eds.), Progress in Physical Geography, 2017.
Sevestre, H., Benn, D.I., 2015. Climatic and geometric controls on the global distribution of surge-type glaciers: implications for a unifying model of surging. J. Glaciol. 61, 646–662. https://doi.org/10.3189/2015JoG14J136.
Springford, A., Eadie, G.M., Thomson, D.J., 2020. Improving the lomb–scargle periodogram with the thomson multitaper. AJ 159, 205. https://doi.org/10.3847/1538-3881/ab7fa1.
Strelin, J.A., Denton, G.H., Vandergoes, M.J., Ninnemann, U.S., Putnam, A.E., 2011. Radiocarbon chronology of the late-glacial puerto bandera moraines, southern patagonian Icefield, Argentina. Quat. Sci. Rev. 30, 2551–2569. https://doi.org/10.1016/j.quascirev.2011.05.004.
Strelin, J.A., Kaplan, M.R., Vandergoes, M.J., Denton, G.H., Schaefer, J.M., 2014. Holocene glacier history of the Lago Argentino basin, southern patagonian Icefield. Quat. Sci. Rev. 101, 124–145. https://doi.org/10.1016/j.quascirev.2014.06.026.
Sugiyama, S., Minowa, M., Sakakibara, D., Skvarca, P., Sawagaki, T., Ohashi, Y., Naito, N., Chikita, K., 2016. Thermal structure of proglacial lakes in Patagonia: proglacial lakes in Patagonia. J. Geophys. Res.: Earth Surf. 121, 2270–2286. https://doi.org/10.1002/2016JF004084.
Van Wyk de Vries, M., Ito, E., Shapley, M., Brignone, G., 2021. Semi-automated counting of complex varves through image autocorrelation: an open-source toolbox. Quat. Res. 104, 89–100.
Van Wyk de Vries, M., Ito, E., Shapley, M., Brignone, G., Wickert, A.D., Miller, L., MacGregor, K.R., 2022. Physical limnology and sediment dynamics of Lago Argentino, the world's largest ice-contact lake. J. Geophys. Res.: Earth Surf. 127.
Villalba, R., Lara, A., Masiokas, M.H., Urrutia, R., Luckman, B.H., Marshall, G.J., Mundo, I.A., Christie, D.A., Cook, E.R., Neukom, R., Allen, K., Fenwick, P., Boninsegna, J.A., Srur, A.M., Morales, M.S., Araneo, D., Palmer, J.G., Cuq, E., Aravena, J.C., Holz, A., LeQuesne, C., 2012. Unusual southern Hemisphere tree growth patterns induced by changes in the southern annular mode. Nat. Geosci. 5, 793–798. https://doi.org/10.1038/ngeo1613.
Visbeck, M., 2009. A station-based southern annular mode index from 1884 to 2005. J. Clim. 22, 940–950. https://doi.org/10.1175/2008JCLI2260.1.
Warren, C.R., 1993. Rapid recent fluctuations of the calving san Rafael glacier, Chilean Patagonia: climatic or non-climatic? Geogr. Ann. Phys. Geogr. 75, 111–125. https://doi.org/10.1080/04353676.1993.11880389.
Zemp, M., Huss, M., Thibert, E., Eckert, N., McNabb, R., Huber, J., Barandun, M., Machguth, H., Nussbaumer, S.U., Gärtner-Roer, I., Thomson, L., Paul, F., Maussion, F., Kutuzov, S., Cogley, J.G., 2019. Global glacier mass changes and their contributions to sea-level rise from 1961 to 2016. Nature 568, 382–386. https://doi.org/10.1038/s41586-019-1071-0.